Published in final edited form as:
Dev Biol. 2012 February 15; 362(2): 219–229. doi:10.1016/j.ydbio.2011.11.011.

Conditional ablation of the *Notch2* receptor in the ocular lens

Senthil S. Saravanamuthu[1], **Tien T. Le**[2], **Chun Y. Gao**[1], **Radu I. Cojocaru**[3], **Pushpa Pandiyan**[4], **Chunqiao Liu**[3], **Jun Zhang**[5], **Peggy S. Zelenka**[1], and **Nadean L. Brown**[2]

[1]Laboratory of Molecular and Developmental Biology, National Eye Institute, National Institutes of Health, Bethesda, MD 20892

[2]Division of Developmental Biology, Cincinnati Children's Hospital Research Foundation, 3333 Burnet Avenue, Cincinnati, OH 45229

[3]Neurobiology Neurodegeneration & Repair Laboratory, National Eye Institute, National Institutes of Health, Bethesda, MD 20892

[4]Laboratory of Immunology, National Institute of Allergy and Infectious Disease, National Institutes of Health, Bethesda MD 20892

[5]Histopathology Core Facility, National Eye Institute, National Institutes of Health, Bethesda, MD 20892

Abstract

Notch signaling is essential for proper lens development, however the specific requirements of individual Notch receptors have not been investigated. Here we report the lens phenotypes of *Notch2* conditionally mutant mice, which exhibited severe microphthalmia, reduced pupillary openings, disrupted fiber cell morphology, eventual loss of the anterior epithelium, fiber cell dysgenesis, denucleation defects, and cataracts. *Notch2* mutants also had persistent lens stalks as early as E11.5, and aberrant DNA synthesis in the fiber cell compartment by E14.5. Gene expression analyses showed that upon loss of *Notch2*, there were elevated levels of the cell cycle regulators *Cdkn1a* (*p21Cip1)*, *Ccnd2* (*CyclinD2*), and *Trp63* (*p63*) that negatively regulates *Wnt* signaling, plus down-regulation of *Cdh1* (*E-Cadherin*). Removal of *Notch2* also resulted in an increased proportion of fiber cells, as was found in *Rbpj* and *Jag1* conditional mutant lenses. However, *Notch2* is not required for AEL proliferation, suggesting that a different receptor regulates this process. We found that *Notch2* normally blocks lens progenitor cell death. Overall, we conclude that *Notch2*-mediated signaling regulates lens morphogenesis, apoptosis, cell cycle withdrawal, and secondary fiber cell differentiation.

Keywords

Notch2; Lens fiber cell differentiation; Lens development; *Jag1*; p21Cip1

Author for Correspondence: Nadean L. Brown, PhD, Division of Developmental Biology, ML 7007, Cincinnati Children's Hospital Research Foundation, 3333 Burnet Avenue, Cincinnati, OH 45229, Voice: 513-636-1963, Fax: 513-636-4317, Nadean.Brown@cchmc.org.

Introduction

The ocular lens develops from invagination of the lens placode within the surface ectoderm, which transforms into a lens vesicle by E10.5 in mice (reviewed in Lovicu et al., 2011). Cells in the posterior vesicle then elongate and terminally differentiate to form lens fiber cells, while the anterior cells maintain a cuboidal epithelial cellular morphology and continue proliferating. These anterior lens progenitor cells constitute the lens growth zone, termed the anterior epithelial layer (AEL). Several growth factor and signaling pathways have been implicated in this process, including *Fgf, Bmp, Wnt* (Belecky-Adams et al., 2002; Boswell et al., 2008; Cain et al., 2008; Chen et al., 2006; Chen et al., 2008; Lovicu and McAvoy, 2005; McAvoy et al., 1999; McAvoy et al., 1991; Stump et al., 2003). The transcription factor, *Foxe3* is initially expressed in all lens vesicle cells, but becomes restricted to AEL by E12.5, along with *Cdh1* (*E-Cadherin*) (Blixt et al., 2000; Brownell et al., 2000; Medina-Martinez et al., 2005; Xu et al., 2002). Thereafter, lens growth and development requires precise control of proliferation and differentiation within the AEL, which contains the progenitor pool for secondary fiber cells that make up bulk of the lens. Differentiated fiber cells express *Cdh2 (N-Cadherin*), *cMaf, Prox1,* and *Cryb, Cryg* (β-, γ-Crystallin)(reviewed in Lovicu et al., 2011). In addition, *Cdkn1c* (*p57Kip2*) is expressed at the early stages of fiber differentiation and serves as a useful marker for the initiation of fiber differentiation (Lovicu and McAvoy, 1999).

Notch signaling is a highly conserved, cell-cell signaling pathway that regulates cell fate determination during development (reviewed in Fortini, 2009; Kopan and Ilagan, 2009). Key components of this pathway include receptors (*Notch1-4*) and ligands (*Deltalike1,3,4, Jag1,2*), which are transmembrane proteins with large extracellular domains. During canonical Notch signaling, ligand binding activates a particular receptor, which undergoes proteolytic cleavage, leading to the release of the C-terminal Notch intracellular domain (NICD). The NICD translocates to the nucleus, where it forms a transcriptional complex with the DNA binding protein Rbpj (RBPJκ), and its co-activator Maml (Mastermind), leading to the activation of target genes. Genes activated by Notch signaling include the *Hes* and *Hey* (*Herp*) family of transcription factors. The *Notch* pathway has a wide variety of functions in both developing and adult tissues. In the developing mouse eye, multiple *Notch* pathway genes are expressed, including *Notch1*, *Notch2*, *Notch3, Jag1, Dll1, Rbpj* and the effector *Hes1* (Bao and Cepko, 1997; Bettenhausen et al., 1995; Ishibashi et al., 1995; Jia et al., 2007; Le et al., 2009; Rowan et al., 2008; Weinmaster et al., 1991). The roles of Notch signaling during lens development and fiber differentiation have only just begun to be understood. Previous studies of *Rbpj* in the lens identified distinct functions for canonical Notch signaling in eye morphogenesis, lens progenitor cell proliferation, transit through the transition zone, and fiber cell differentiation (Jia et al., 2007; Rowan et al., 2008). In addition, conditional deletion of either *Rbpj* (Jia et al., 2007; Rowan et al., 2008) or *Jag1* (Le et al., 2009), suggested cell cycle regulatory genes like *Ccnd1* (*CyclinD1*), *Ccnd2* (*CyclinD2*), *Cdkn1b* (*p27Kip1*) and/or *Cdkn1C* (*p57Kip2*), may be regulated by Notch signaling during the decision of lens progenitor cells to divide further versus differentiate.

While these studies clearly demonstrated the importance of Notch signaling in the developing lens, it is unknown when and where specific receptors act, including whether they exhibit distinct functions. The first suggestion of a specific role was provided by a global gene profiling study comparing mRNA expression between human lens epithelial cells and cortical fiber cells, which found that *Notch2* expression was significantly higher in the epithelium (Hawse et al., 2005). In vitro studies of postnatal rat lens epithelial differentiation demonstrated that *Notch2* signaling is activated during FGF-dependent secondary fiber cell differentiation (Saravanamuthu et al., 2009). No corresponding activation of *Notch1* was detected, but the unique requirements of *Notch2* were not

investigated further. In this study we used the Le-Cre driver to conditionally delete the *Notch2* receptor during mouse lens development. *Jag1* and *Rbpj* were previously shown to act during lens vesicle morphogenesis, AEL progenitor cell proliferation and fiber cell differentiation. Here, our results indicate that although the lens-specific loss of *Notch2* phenocopies the absence of *Rbpj* or *Jag1* during vesicle morphogenesis and fiber cell differentiation, *Notch2* is not required for proliferation in the lens. Instead, we find that this receptor uniquely blocks lens cell apoptosis.

Materials and Methods

Animals

Notch2$^{CKO/CKO}$ mice were obtained from Tom Gridley and genotyped using published protocols (McCright et al., 2006). Throughout this paper the abbreviation CKO indicates a "Conditional Knockout Allele". *Le-Cre* mice were obtained from Dr. Joram Piatigorsky and Ruth Ashery-Padan, and genotyped according to published protocols (Ashery-Padan et al., 2000). All mice were housed and cared for in accordance with the guidelines provided by the National Institutes of Health, Bethesda, MD and the Association for Research in Vision and Ophthalmology.

Tissue analysis

Embryonic and postnatal tissues were fixed in 4% paraformaldehyde/PBS for 1–2 hours at 4°C, processed through a sucrose/PBS series, cryoembedded and 10 micron sections generated. Primary antibodies used were anti-BrdU (Serotec clone BU1/75 1:100), anti-cPARP (Cell Signaling 1:500), anti-Ccnd2 (Santa Cruz 34B1-3 1:200), anti-Cdh1(Zymed ECCD-2 1:500), anti-Foxe3 (gift from Peter Carlsson 1:1000), anti-Cryb (gift from Richard Lang 1:8000), anti-Crya (gift from Eric Wawrousek 1:1000), anti-Cryg (Santa Cruz SC22415, 1:1000), anti-GFP (Molecular Probes 1:1000), anti-Hes1 (1:1000), anti-Jag1 (Santa Cruz 1:1000), anti-Cdkn1c (Abcam 1:200), anti-Prox1 (Covance 1:6000), anti-Cdh2 (BD Transduction Laboratories, 1:100), and anti-cMaf (Santa Cruz 1:200). Secondary antibodies were directly conjugated to Alexa Fluor 488, Alexa Fluor 594 (Invitrogen) or biotinylated (Jackson Immunologicals) and sequentially labeled with Alexa 488- or 594-Streptavidin (Invitrogen), followed by DAPI nuclear labeling. Microscopic imaging was performed on a Zeiss fluorescent microscope with a Zeiss camera and Apotome deconvolution device. For S-phase analyses, BrdU (Sigma) was injected intraperitoneally and animals sacrificed 1.5 hours later for tissue processing, following the method of (Mastick and Andrews, 2001). Standard histology on paraffin embedded sections was also performed. Images were processed using Axiovision (v7.0) and Adobe Photoshop (CS4) software and electronically adjusted for brightness, contrast and pseudocoloring.

Cell Counting

Tissue sections, separated by at least 60 μm, were antibody-stained and counted using NIH ImageJ or Axiovision software. At least two independent sections from each animal, using 3 or more mice per genotype and age were quantified. Labeling indices for BrdU+, Foxe3-neg or cPARP+ cells were generated by dividing the number of antibody-positive cells by total DAPI-labeled nuclei, and compared against one other genotype using a two-tailed, unpaired Student T-Test, to determine p values.

Transmission Electron Microscopy

Lens were removed from E14.5 mice and fixed in 2% glutaraldehyde and 2% paraformaldehyde in 0.1 M sodium phosphate buffer (PB), pH 7.4 for 12 h at room temperature (RT). After a wash with rinsing buffer (RB, 4% sucrose and 0.15 mM CaCl2 in

PB), pH 7.4 at 4°C, tissues were postfixed in 1% OsO4 in 0.1 M PB, pH 7.4 for 1 h. After rinsing and dehydration, tissues were embedded in Epon 812 for 72 h at 60°C. One micron semi-sections were used for tissue orientation. Then 70–90 nm ultrasections were collected in 200 mesh grids and counterstained with 5% uranyl acetate and 0.3% lead citrate. Sections were viewed on a JEOL 1010EM at 60 KV and digital images were acquired at 2000–10,000X magnifications by AMT software (Advanced Microscopy Techniques, Corp.).

In situ Hybridization

In situ hybridization was performed on frozen mouse embryonic sections. RNA probe labeling and in situ hybridization were performed essentially as described (Rosen and Beddington, 1993). Embryos were snap frozen, cryosectioned, post-fixed, washed with PBS, prehybridized and then hybridized overnight at 66°C. Post-hybridization steps were carried out as described (Rosen and Beddington, 1993). The template was a 554bp region in the UTR of *Notch2* (NCBI NM_010928) similar to the one described for rat *Notch2* in (Lindsell et al., 1996). The template was amplified such that the sequence for the T7 bacteriophage promoter was built into the reverse primer sequence (Forward: 5′-GGGCCCGGAAYYCTCCACCTGCATTGACCGCGTGGCC-3′, Reverse: 5′-GGGCCCGGAATTCGTCATCAATGTCGATCTGGCACACTGGTCC-3′).

Lens homogenate preparation for FACS analyses

Intact lenses from E14.5 embryos were isolated into M199 medium. Medium was aspirated slowly to resuspend them in 1 ml of HBSS (Ca++ and Mg++ free). HBSS was slowly aspirated off and 100ul of collagenase solution was added. The collagenase digestion was carried out at 37°C using 3.4 U collagenase H (Sigma) in HBSS with 10% FCS. After collagenase digestion, the lenses were homogenized and resuspended using 200ul pipette tip. Then 1ml of PBS was added and the cells were washed with PBS by spinning at 1400rpm at 4°C for 5 min. Adult lens cells were passed through 100um strainer before washing.

Fixation and Staining for FACS analysis

The cell pellet was resuspended with pulse vortex by adding 1 ml of freshly prepared Fixation/Permeabilization working solution (E Biosciences). They were incubated at 4°C for 18 hours in the dark, followed by washing with 2 ml 1X Permeabilization Buffer. After decanting the supernatant the cells were blocked with 5% FCS in 1X Permeabilization Buffer, (Ebiosciences) in approximately 100 μl volume, at 4°C for 15 minutes. This was followed by washing cells with 2 ml 1X Permeabilization Buffer. Then the antibodies were added at required working concentrations in 1X Permeabilization buffer and the cells were incubated in the antibody solution at 4°C for at least 30 minutes in the dark. This was followed by washing the cells with 2 ml 1X Permeabilization Buffer. Then they were resuspended in 300ul volume PBS/BSA (0.5%) buffer and analyzed on FACS Calibur (BD Biosciences) cytometer. For cell counting 50ul (50,000 beads) of Countbright beads (Invitrogen) were added just before acquisition in the flow cytometer.

DNA microarray analysis

Intact lenses were dissected from three *Notch2*$^{CKO/CKO}$ controls and three Le-Cre; *Notch2*$^{CKO/CKO}$ mutant mice at E19.5 and the two lenses of every animal were pooled together. Total RNA was isolated using Trizol reagent (Invitrogen). Microarray data was collected at Expression Analysis, Inc. (www.expressionanalysis.com; Durham, NC). Before target production, the quality and quantity of each RNA sample was assessed using a 2100 BioAnalyzer (Agilent). Target was prepared and hybridized according to the “GeneChipR 3′ IVT Express Kit User Manual” using the reagents provided in the GeneChipR 3′ IVT Express Kit (Affymetrix Part#901228). The microarrays were then stained with Streptavidin

Phycoerythrin and the fluorescent signal was amplified using a biotinylated antibody solution. Fluorescent images were detected in a GeneChip® Scanner 3000 and expression data was extracted using the GeneChip Operating System v 1.1 (Affymetrix). All GeneChips were scaled to a median intensity setting of 500. An estimate of signal for each transcript was calculated using the Microarray Suite Algorithm version 5.0 (Affymetrix) using the Expression Console version 1.1 (Affymetrix). The values of individual probes belonging to one probe set were averaged and normalized using GeneSpring v11.0.2 (Agilent Technologies Inc., Palo Alto, CA, USA). The average fluorescence intensity of all annotated gene was calculated using Robust Multi-array Analysis (RMA) algorithm. In order to identify differentially expressed genes between the two conditions, a one-way Analysis of Variance (ANOVA) was performed. Only genes with an uncorrected p-value less than 0.01 were used, ending up with 1299 probes. From this set of genes, 44 probes (32 genes) had a greater than 3-fold change. (GEO Accession Number GSE31643).

Quantitative real time PCR (RT-qPCR) analysis

RT-qPCR analysis was performed using SABiosciences/Qiagen qPCR arrays using reagents supplied by the manufacturer. Total RNA was isolated from E19.5 lenses using RNeasy Micro kit (Qiagen). RT-qPCR was performed using qPCR arrays PAMM-043A (Wnt pathway), PAMM-020 (Cell cycle pathway) and PAMM-059 (Notch pathway) purchased from SA Biosciences, Qiagen according to manufacturer's instructions. A 7900 HT real time PCR instrument (Applied Biosystems) and SDS2.3 software were used to collect run data and threshold cycle (Ct) values of individual reactions. Further data analysis was carried out using Microsoft Excel based worksheets or online data analysis software found at www.sabiosciences.com.

Results

Notch2 mRNA expression during lens development

Previous studies reported that *Notch* receptors are expressed in the lens, ciliary body, RPE and retina of embryonic mice (Bao and Cepko, 1997; Weinmaster et al., 1991), and *Notch2* in particular, is present in the newborn rat lens epithelium (Saravanamuthu et al., 2009). However, the spatiotemporal expression pattern of *Notch2* in the developing rodent lens has not been systematically examined. To better understand the potential role of *Notch2* during lens development, we examined mRNA expression at various stages of lens development by in situ hybridization. At embryonic day 11.5 (E11.5) expression of *Notch2* is mostly localized within the retinal pigmented epithelium (RPE) (Fig. 1A). At E13.5 *Notch2* expression is detected in the lens vesicle, predominantly in the anterior epithelial layer (AEL) (Fig. 1B). By E16.5, *Notch2* mRNA is present in both the AEL and transition zone (TZ), around the lens equator (Fig. 1C), as well as in the RPE. At postnatal day 3 (P3), *Notch2* lens expression remains confined to the AEL and transition zone (Fig. 1D). The corneal epithelium shows no detectable levels of *Notch2* mRNA while non-neuronal eye cup derivatives, including the RPE, iris, and ciliary tissue, also express *Notch2*, consistent with previous reports (Bao and Cepko, 1997). In addition, we also observed *Notch2* expression in skin hair follicles of the eyelids, as previously reported (Schouwey et al., 2007).

Conditional ablation of *Notch2* in the developing lens causes microphthalmia

To remove *Notch2* in the developing mouse lens, we used Le-Cre mediated recombination of a Notch2 floxed allele (Ashery-Padan et al., 2000; McCright et al., 2006) (Fig. 2A). Adult Le-Cre*; Notch2*$^{CKO/CKO}$ mice showed severe microphthalmia, accompanied by reduced or absent pupillary openings (Fig. 2B-E) compared to *Notch2*$^{CKO/CKO}$ controls (n = 3). Since the Le-Cre transgene has an IRES-GFP expression cassette, GFP fluorescence serves as an indicator of Cre expression. Fig. 2G shows specific GFP expression in E11.5 Le-Cre*;*

Notch2$^{CKO/CKO}$ lens vesicles, compared to background fluorescence in littermate *Notch2*$^{CKO/CKO}$ controls (Fig. 2F).

Histological analysis of 10 weeks old adult Le-Cre*; Notch2*$^{CKO/CKO}$ eyes showed a severely deformed lens with extensive vacuoles, unlike the control lenses (Fig. 3A,B). Heterozygous Le-Cre; *Notch2*$^{CKO/+}$ eyes had no obvious phenotype (Supplementary Fig. S1). Importantly, the adjacent cornea, which does not normally express *Notch2* mRNA (Fig. 1D), was unaffected in Le-Cre*; Notch2*$^{CKO/CKO}$ (Fig. 3C,D). However, in addition to an abnormal AEL, Le-Cre*; Notch2*$^{CKO/CKO}$ mutants also displayed fused irises and defective pupillary eye openings (Fig. 3E,F). Defects in the transition zone of the Le-Cre*; Notch2*$^{CKO/CKO}$ lenses include abnormal distribution of nuclei, globular fiber morphology, inappropriate nucleated fiber cells along the posterior capsule defective fiber cell elongation (Fig. 3G–J).

Loss of *Notch2* results in persistent lens stalks, microphthalmia and aberrant lens morphology during embryonic development

To define better the onset of defects in the lens, due to loss of *Notch2*, we compared the morphology of *Notch2*$^{CKO/CKO}$ controls and Le-Cre*; Notch2*$^{CKO/CKO}$ mutants, during prenatal development. H&E staining of histological sections of E12.5 Le-Cre*; Notch2*$^{CKO/CKO}$ mutant embryonic eyes showed a reduced lens vesicle, with incomplete separation from the surface ectoderm (Fig. 4A,B). This defective separation resulted in a persistent lens stalk, as highlighted by colabeling for Foxe3 (red) and Cdh1 (E-Cadherin, green) (Fig 4C,D see insets). Immunofluorescence staining of the *Notch* effector, Hes1, demonstrated that this protein has been downregulated, compared to *Notch2*$^{CKO/CKO}$ controls (Fig. 4E,F). Primary fiber cell elongation appeared normal and elongating cells expressed characteristic proteins, such as Jag1 (Fig. 4G,H), Cryb (β-Crystallin) (Fig. 4I,J), Ccnd2 and cMaf (Fig 4 K,L), supporting the idea that *Notch2* has little if any role in primary fiber genesis.

At E14.5 Le-Cre; *Notch2*$^{CKO/CKO}$ lenses were distinctly microphthalmic (Fig 5A,G). Both the extent and thickness of the AEL were reduced and nuclei of the peripheral lens fibers failed to form a pronounced “bow”, suggesting a possible defect in elongation of the secondary fiber cells (Fig. 5A,B,G,H). Immunostaining for the Notch ligand, Jag1, was detected along the surface membranes of newly formed secondary fibers of both *Notch2*$^{CKO/CKO}$ control and Le-Cre; *Notch2*$^{CKO/CKO}$ mutant lenses; however, mutant secondary fiber cells were small and poorly elongated (Fig. 5C,I). Expression of the *Notch* effector Hes1 was detected in only a few, isolated cells in the AEL of Le-Cre; *Notch2*$^{CKO/CKO}$ mutant lenses (arrows in Fig. 5D,J). The anterior lens epithelium (AEL) marker Foxe3 was detected in most AEL cells, although occasional Foxe3-negative cells were observed (Fig. 5E,K). Ccnd2, which is normally upregulated in the transition zone (Fromm and Overbeek, 1996), was appropriately expressed in the corresponding cells of the Le-Cre; *Notch2*$^{CKO/CKO}$ mutant (Fig. 5E,K). Cdh1 expression was normal in the AEL of the Le-Cre; *Notch2*$^{CKO/CKO}$ mutant and properly downregulated in the elongating fibers (Fig. 5F,L). Moreover, Cdh1 expression in the AEL illustrated a reduced AEL thickness, as well as the persistence of a lens stalk (arrow in L). The transcription factor Prox1, like Jag1 and Ccnd2, is normally upregulated in the transition zone and differentiating fibers (Fromm and Overbeek, 1996; Le et al., 2009; Wigle et al., 1999), was also expressed appropriately in nuclei of both the primary and secondary fiber cells (Fig 5F,L). The loss of *Notch2* did not affect the onset of the differentiation markers assayed, within the posterior fiber cell compartment. However, subsequent lens fiber cell morphology, particularly elongation, was abnormal.

Aberrant proliferation of fiber cells in Le-Cre; *Notch2*$^{CKO/CKO}$ mutant lenses

To determine whether conditional deletion of *Notch2* reduces AEL proliferation, as has been reported for *Rbpj* and *Jag1* mutant lenses (Jia et al., 2007; Le et al., 2009; Rowan et al., 2008), we BrdU pulse-labeled embryonic lenses at E11.5 and E14.5. Interestingly, there was no significant difference in the percentage of BrdU+ S-phase cells in Le-Cre;*Notch2*$^{CKO/CKO}$ and *Notch2*$^{CKO/CKO}$ lenses, at either age (Figs. 6A,B,E), indicating that *Notch2* is not required for AEL proliferation. In addition, a number of S-phase nuclei were apparent in the fiber cell compartment of *Notch2* mutant lenses, suggesting a defect in cell cycle withdrawal during differentiation (arrow in Fig. 6B). Since BrdU+ cells are occasionally found in the posterior compartment of the normal prenatal mouse lens, we carefully quantified the number of BrdU+ fiber cells (that were Cdh1 negative) in multiple sections of *Notch2*$^{CKO/CKO}$ and Le-Cre*;Notch2*$^{CKO/CKO}$ lenses. The results showed a significantly larger proportion of BrdU+ fiber cells in the absence of *Notch2* (Fig. 6F), suggesting that *Notch2* normally promotes cell cycle withdrawal during secondary fiber cell formation.

To investigate the cell cycle status of the differentiating secondary fibers further, we used flow cytometry to identify cells in the early stages of secondary fiber cell formation. Such cells can be recognized by the progressive loss of Cdh1, which indicates the onset of fiber differentiation (Saravanamuthu et al., 2009; Xu et al., 2002). Fluorescent Activated Cell Sorting (FACS) of E14.5 lens cell preparations was used to enrich Cdh1+ lens epithelial cells and identified about 55 – 70% (n=3 experiments) of the cells as the Cdh1+ population (compare Figs. 7A and 7B, data not shown). The increased sensitivity of this FACS assay distinguished two sub-populations of Cdh1+ cells, one showing high expression, the other with low expression (Fig. 7C). The high Cdh1+ cells had 15-fold higher fluorescence intensity than the low Cdh1+ cells, and were represented by two distinct peaks of fluorescence intensity. To confirm that the Cdh1+ cells were derived from the lens, two populations of cells were also tested for the lens specific marker, Crya (α-Crystallin). The results demonstrated that all the Cdh1+ cells from the embryonic lens preparation were all also positive for lens marker Crya, thereby confirming that they derived from the lens, and not contaminating tissues (data not shown). Forward scatter parameter in the FACS assay distinguishes cells based on their size, and to lesser extent cell shape. Forward scatter of the high expresser Cdh1+ population indicated a larger, more rounded cell profile typical of epithelial cells. In contrast, the forward scatter of the low expressers indicated a smaller size and likely flattened cell shape, consistent with the cell elongation that occurs in the early stages of fiber cell differentiation (Fig 7D,E). Thus, we consider the low expresser Cdh1+ population to represent cells that have begun to lose Cdh1 expression and elongate at the lens equator. Examining this low Cdh1+ population for BrdU labeling revealed that Le-Cre*;* *Notch2*$^{CKO/CKO}$ mutant lenses harbored a significantly higher percentage of BrdU+ cells (Fig. 7F). This supports the view that *Notch2* deletion leads to aberrant cell cycle withdrawal during differentiation.

Abnormal accumulation of Foxe3-negative cells in Le-Cre*; Notch2*$^{CKO/CKO}$ lenses

Lenses deficient in *Rbpj* or *Jag1* showed an excess of differentiated fiber cells, as seen by a larger than normal percentage of Foxe3-negative cells at E11, E12.5, and E14.5 (Le et al., 2009; Rowan et al., 2008). To examine whether Le-Cre*; Notch2*$^{CKO/CKO}$ mutant lenses exhibit the same phenotype, we quantified the percentage of Foxe3-negative cells at E11.5 and E14.5 (Fig. 6G). There was no significant difference in this population at E11.5, but at E14.5 *Notch2* lens mutants had a significant increase in the proportion of fiber cells. Paradoxically, there was no corresponding increase in cell proliferation during this period, suggesting that the increase in fiber cells might be balanced by a loss of AEL cells through apoptosis in the absence of *Notch2*. To test this possibility, the percentage of cPARP+

(caspase 3 cleavage product of polyADP-ribose polymerase) AEL cells was quantified (Figs 6C,D,H). The results showed that 1.1% of AEL cells were apoptotic in Le-Cre*; Notch2*$^{CKO/CKO}$ lenses, compared to zero in *Notch2*$^{CKO/CKO}$ controls. Thus, Le-Cre*; Notch2*$^{CKO/CKO}$ mutant lenses have a significantly higher rate of apoptosis in the AEL.

At older ages the AEL of Le-Cre*; Notch2*$^{CKO/CKO}$ mutants was even further reduced in size, as revealed by Cryb (Fig. 8A,F) *Foxe3* (Fig. 8B,G) or Cdh1 (Fig. 8C,H,E,J) expression. Moreover, few cells were positively stained for the early differentiation marker Cdkn1c (Fig. 8E,J)(Zhang et al., 1998), indicating a defective transition zone in the Le-Cre*; Notch2*$^{CKO/CKO}$ mutant lenses. However, Cryb immunofluorescence revealed a loss of parallel arrangement of fibers and defective fiber elongation in the mutant (Fig. 8F). Late expression of Jag1 and Cdh2, were abnormal in Le-Cre*; Notch2*$^{CKO/CKO}$ mutant lenses, with only a few positively stained cells observable (Fig. 8B,G and 8D,I). As further evidence of fiber cell disorder, staining for Prox1 revealed fiber disorders in the *Notch2* mutants (Fig. 8C,H).

Gene expression changes associated with Le-Cre; *Notch2*$^{CKO/CKO}$ lenses

To identify specific genes that may be affected by *Notch2* deletion, we compared gene expression profiles across three biological replicates of E19.5 *Notch2*$^{CKO/CKO}$ (control) and Le-Cre; *Notch2*$^{CKO/CKO}$ (mutant) lenses, using Affymetrix mouse genome 430 2.0 arrays. Forty-four transcripts were identified as being elevated or reduced by at least 3-fold (as compared to controls) with p-values<0.001. A heat map distribution of fold change patterns of the top differentially expressed genes is shown in Fig. 9. A complete list of identified transcripts corresponding to these genes and their fold changes is provided in Supplemental Table 1. Genes that were significantly upregulated in the Le-Cre*; Notch2*$^{CKO/CKO}$ mutant lenses included *Fgf12, Fgf15*, which is noteworthy because multiple Fgf factors induce lens fiber cell differentiation; *Cdkn1a* (p21Cip1), which is involved in cell cycle control (Xiong et al., 1993); and two genes involved in thyroid hormone signaling, the thyroid binding protein *Crym* (μ-Crystallin) (Finckh et al., 1998), and the thyroid hormone responsive spot 14, *Thrsp* (Zhu et al., 2005; Zhu et al., 2001). Downregulated genes included the epithelial cell junctional protein, *Cdh1*, *Olfml3* (olfactomedin-like3), which has been implicated in Bmp regulation (Inomata et al., 2008), *Dnase2b*, which is involved in fiber cell denucleation (Nishimoto et al., 2003; Torriglia et al., 1995), and the *Pdgfra* receptor, which regulates AEL cell proliferation (Kok et al., 2002).

As an independent approach to identifying gene expression differences between Le-Cre*; Notch2*$^{CKO/CKO}$ mutant lenses and *Notch2*$^{CKO/CKO}$ control lenses, we used real time qPCR arrays focused on genes associated with proliferation and differentiation. These included genes in the Notch and Wnt signaling pathways, and cell cycle regulatory genes. Expression of 252 genes involved in one or more of these three pathways were analyzed. The qPCR outcomes for genes with at least 1.5-fold differential expression between control and *Notch2* conditional mutant lenses (p value <0.05) are listed in Table 1. The most strongly upregulated gene identified by this method was the transformation related protein *Trp63*. Other upregulated genes included cell cycle regulatory genes such as *Ccnd2*, and three cyclin-dependent kinase inhibitors, *Cdkn1a* (*p21Cip1*), *Cdkn1c* (*p57Kip2*), and *Cdkn2a* (*p16Ink4*). Multiple Wnt pathway genes were also upregulated, including *Wnt16* and *Wnt8b*; Wnt inhibitors *Dkk1*, *Sfrp4*; the Wnt receptor *Fzd8*; a Wnt pathway antagonist, *Pparg* (PPAR-gamma) and Wnt target genes *Tcf7*, *Tle1*, *Tle2*, and *Wisp1*. A number of genes were also downregulated, including *Wnt4*, *Wnt7b*, and the secreted frizzled-related protein, *Sfrp1*, which inhibits Wnt signaling, as well as *Cdh1*. These changes in gene expression provide candidates that may play a role in specific features of the Le-Cre; *Notch2*$^{CKO/CKO}$ mutant phenotype, such as loss of AEL, defective cell cycle withdrawal, and aberrant fiber cell differentiation.

Discussion

Our findings show that *Notch2* function is essential for prenatal lens development and differentiation. Conditional deletion of *Notch2* causes a persistent lens stalk, followed by a progressive loss of the AEL and transition zone, disruption of secondary fiber cell differentiation, and apoptosis. Although in the absence of *Notch2*, fiber cell markers had normal spatiotemporal expression patterns, we found that secondary lens fibers failed to elongate, and properly withdraw from the cell cycle.

Lens progenitor cell requirement for Notch2

At the outset, we predicted that *Notch2* lens mutants would have reduced AEL cell proliferation, like *Jag1* and *Rbpj* conditional mutants. This was not the case, although *Notch2* embryonic mutant lenses are smaller than controls. Instead, we found aberrant S-phase fiber cells. Our FACS analysis confirmed that *Notch2* mutant lenses have a significant increase in a low Cdh1-expressing population, which are initiating fiber cell differentiation, yet also inappropriately contain more BrdU+ cells. This could occur if *Notch2* mutant cells undergo longer cell cycles, or are unable to fully exit mitosis. We favor the former idea, since mutant fiber cells activate the expression of multiple postmitotic and terminal differentiation markers at the appropriate time and place.

Proper lens vesicle closure and separation from the overlying ectoderm depends on the *Foxe3* transcription factor (Blixt et al., 2000; Brownell et al., 2000; Medina-Martinez et al., 2005; Medina-Martinez and Jamrich, 2007). *Foxe3* is expressed in all lens vesicle cells until E12, when it becomes restricted to the AEL. *Foxe3* mutant lenses are microphthalmic with persistent lens stalks, like *Notch2* conditional mutants. Thus, Notch signaling and *Foxe3* act similarly in the lens, further supported by a significant loss of Foxe3+ AEL cells in E14.5 *Notch2* mutants. *Foxe3* mutant lenses have reduced *Dnase2b* expression, which regulates fiber cell denucleation (Counis et al., 1998; Torriglia et al., 1995), and *Pdgfra*, which promotes AEL proliferation (Kok et al., 2002). Interestingly both of these genes were downregulated in the Le-Cre*; Notch2*$^{CKO/CKO}$ mutant lenses. Although this might suggest that *Foxe3* is regulated by a Jag1-Notch2-Rbpj signal, this issue is unresolved, since *Foxe3* initiates normally in the lens of each Notch pathway mutant. Alternatively, *Foxe3* lens expression requires activation of *Smad8* (Yoshimoto et al., 2005) which could theoretically interact with the Notch2 intracellular domain (N2-ICD), for noncanonical *Notch* functions, as was reported for N1-ICD and Smad3 (Blokzijl et al., 2003). In addition, we found that Le-Cre; *Notch2*$^{CKO/CKO}$ lenses have depressed levels of Olfml-3, a protein that promotes Bmp signaling in *Xenopus* (Inomata et al., 2008). Reduced levels of Olfml-3 would be expected to reduce Bmp signaling, Smad8 activation, and Bmp-dependent *Foxe3* expression.

However, none of these gene expression changes can fully account for the small lens phenotype of *Notch2* conditional mutants. Instead, we found *Notch2*-specific defects that might (separately or together) cause microphthalmic lenses. The persistent lens stalks of *Notch2* mutants could trap progenitor cells, causing a progressive loss of proliferation, but with no significant loss of proliferation in *Notch2* lens mutants, we do not favor this possibility. Instead, there is increased apoptosis in the absence of *Notch2*. Putative downstream genes that link *Notch2* activity to the regulation of cell death were not identified; making this is a good starting point for future studies.

Notch2 function during lens fiber cell differentiation

The inappropriate S-phase fiber cells might arise from elevated expression of the transformation related protein, *Trp63*, in Le-Cre*; Notch2*$^{CKO/CKO}$ mutants. This protein has context-specific functions, since it has been linked with prolonged proliferation and aberrant

differentiation, can either block or promote apoptosis, can act downstream of *Wnt9b* signaling, or negatively regulate other components of the *Wnt* pathway (Drewelus et al., 2010; Ferretti et al., 2011; Talos et al., 2010). In addition, our gene expression data indicated that the cell cycle inhibitor, Cdkn1a (p21Cip1), was upregulated in Le-Cre*; Notch2*$^{CKO/CKO}$ lenses (Fig. 9, Table1). When Cdkn1a is overexpressed, it can promote Fgf-dependent cell cycle progression, by favoring the assembly of active Cdk4/CyclinD complexes (Bansal et al., 2005). The derepression of Ccnd2 and Fgf isoforms in the Le-Cre*; Notch2*$^{CKO/CKO}$ lenses might further enhance this process, particularly in the absence of counterbalancing expression of cell cycle inhibitors (Fig 9, Table1). As a whole, our findings support the idea that *Notch2* normally promotes cell cycle withdrawal.

Conditional deletion of *Notch2* also had a marked effect on secondary fiber cell elongation and morphology. Instead of forming a regular array of closely adherent, elongated cells, secondary fiber cells of the Le-Cre; *Notch2*$^{CKO/CKO}$ mutant were randomly arranged and globular. Similar, abnormal fiber morphology occurs in lenses deficient in *Itgb1* (β1-Integrin) (Simirskii et al., 2007), an adhesion protein normally present on basolateral surfaces of lens fiber cells (Menko and Philip, 1995; Walker and Menko, 2009), raising the possibility that *Notch2* may play a role in *Itgb1*-dependent cell-cell adhesion in lens fiber cells. Interestingly, a non-canonical effect of the Notch intracellular domain has been shown to promote activation of *Itgb1* by binding to, and activating Rras, thus reversing the Hras mediated suppression of integrin affinity (Karsan, 2008). Both Rras and Hras are expressed in lens fiber cells and overexpression of active Hras in the lens disrupts lens development (Reneker et al., 2004). Together, the aberrant fiber cell morphology and defective cell cycle withdrawal of secondary fiber cells in *Notch2* deficient lenses demonstrate that *Notch2* is essential for proper secondary lens fiber cell differentiation, as previous in vitro experiments have already demonstrated (Saravanamuthu et al., 2009).

Towards an understanding of Notch signaling in the mouse lens

When the *Notch2* lens phenotypes are integrated with those *Jag1* and *Rbpj* conditional mutants (Jia et al., 2007; Le et al., 2009; Rowan et al., 2008), a somewhat complex picture of Notch signaling emerges for the developing lens. First, during mouse lens induction and vesicle formation, Notch signaling has only a minor role, during vesicle separation from the overlying ectoderm. All other aspects of early lens development: specification, vesicle growth, morphogenesis and primary fibergenesis, occur independent of this pathway. However, a Jag1-Notch2-Rbpj mediated signal is necessary for proper secondary fiber formation. Loss of any gene results in *Hes1* downregulation, progressive dysgenesis of the AEL and transition zone, and a failure of fiber cell denucleation.

Interestingly, *Jag1* lens mutants phenocopy those for *Rbpj*, particularly a loss of AEL cell proliferation. Although we found the *Notch2* receptor is not required for this process, it does uniquely block apoptosis. Furthermore, *Rbpj* and *Jag1* are also required for some aspect of secondary fiber cell differentiation, but the nature of this abnormality was not apparent in those mutants, since proliferation and differentiation simultaneously arrested. By contrast, Le-Cre; *Notch2*$^{CKO/CKO}$ mutant lenses retain AEL cell proliferation, which allowed defective fiber cells to accumulate in the posterior compartment, making their inability to fully exit mitosis obvious. The distinct phenotypes among these three genes strongly suggest additional ligands, receptors and downstream effectors are involved in midgestational and postnatal lens development. In particular, the *Dll1* ligand, *Notch1* and *Notch3* receptors are each expressed during rodent lens development (Bao and Cepko, 1997; Weinmaster et al., 1991; Le and Brown, unpublished data). Therefore, Notch signal transduction appears to segregate its regulation of particular cell processes (e.g. proliferation versus apoptosis) among distinct ligand and receptor combinations. Alternatively, as already mentioned, there

may be additional, noncanonical functions for some or all of these genes during lens formation. It will be very interesting in the future to unravel these questions.

Supplementary Material

Refer to Web version on PubMed Central for supplementary material.

Acknowledgments

The authors thank Tom Gridley for Notch2$^{CKO/CKO}$ mice; Ruth Ashery-Padan and Joram Piatigorsky for Le-Cre transgenic mice; Richard Lang for Cryb antibody; Peter Carlsson for Foxe3 antibody; Eric Wawrousek for Crya antibody, Barbara Norman for technical expertise; and Richard Lang and Tiffany Cook for valuable discussion. This work was supported by the National Eye Institute Intramural Research Program Z01-EY000238 to PSZ and NIH R01 grant EY18097 to NLB.

References

Ashery-Padan R, Marquardt T, Zhou X, Gruss P. Pax6 activity in the lens primordium is required for lens formation and for correct placement of a single retina in the eye. Genes Dev. 2000; 14:2701–11. [PubMed: 11069887]

Bansal R, Marin-Husstege M, Bryant M, Casaccia-Bonnefil P. S-phase entry of oligodendrocyte lineage cells is associated with increased levels of p21Cip1. J Neurosci Res. 2005; 80:360–8. [PubMed: 15789403]

Bao ZZ, Cepko CL. The expression and function of Notch pathway genes in the developing rat eye. J Neurosci. 1997; 17:1425–34. [PubMed: 9006984]

Belecky-Adams TL, Adler R, Beebe DC. Bone morphogenetic protein signaling and the initiation of lens fiber cell differentiation. Development. 2002; 129:3795–802. [PubMed: 12135918]

Bettenhausen B, Hrabe de Angelis M, Simon D, Guenet JL, Gossler A. Transient and restricted expression during mouse embryogenesis of Dll1, a murine gene closely related to Drosophila Delta. Development. 1995; 121:2407–18. [PubMed: 7671806]

Blixt A, Mahlapuu M, Aitola M, Pelto-Huikko M, Enerback S, Carlsson P. A forkhead gene, FoxE3, is essential for lens epithelial proliferation and closure of the lens vesicle. Genes Dev. 2000; 14:245–54. [PubMed: 10652278]

Blokzijl A, Dahlqvist C, Reissmann E, Falk A, Moliner A, Lendahl U, Ibanez CF. Cross-talk between the Notch and TGF-beta signaling pathways mediated by interaction of the Notch intracellular domain with Smad3. J Cell Biol. 2003; 163:723–8. [PubMed: 14638857]

Boswell BA, Overbeek PA, Musil LS. Essential role of BMPs in FGF-induced secondary lens fiber differentiation. Dev Biol. 2008; 324:202–12. [PubMed: 18848538]

Brownell I, Dirksen M, Jamrich M. Forkhead Foxe3 maps to the dysgenetic lens locus and is critical in lens development and differentiation. Genesis. 2000; 27:81–93. [PubMed: 10890982]

Cain S, Martinez G, Kokkinos MI, Turner K, Richardson RJ, Abud HE, Huelsken J, Robinson ML, de Iongh RU. Differential requirement for beta-catenin in epithelial and fiber cells during lens development. Dev Biol. 2008; 321:420–33. [PubMed: 18652817]

Chen Y, Stump RJ, Lovicu FJ, McAvoy JW. A role for Wnt/planar cell polarity signaling during lens fiber cell differentiation? Semin Cell Dev Biol. 2006; 17:712–25. [PubMed: 17210263]

Chen Y, Stump RJ, Lovicu FJ, Shimono A, McAvoy JW. Wnt signaling is required for organization of the lens fiber cell cytoskeleton and development of lens three-dimensional architecture. Dev Biol. 2008; 324:161–76. [PubMed: 18824165]

Counis MF, Chaudun E, Arruti C, Oliver L, Sanwal M, Courtois Y, Torriglia A. Analysis of nuclear degradation during lens cell differentiation. Cell Death Differ. 1998; 5:251–61. [PubMed: 10200471]

Drewelus I, Gopfert C, Hippel C, Dickmanns A, Damianitsch K, Pieler T, Dobbelstein M. p63 antagonizes Wnt-induced transcription. Cell Cycle. 2010; 9:580–87. [PubMed: 20107313]

Ferretti E, Li B, Zewdu R, Wells V, Hebert JM, Karner C, Anderson MJ, Williams T, Dixon J, Dixon MJ, Depew MJ, Selleri L. A Conserved Pbx-Wnt-p63-Irf6 Regulatory Module Controls Face

Morphogenesis by Promoting Epithelial Apoptosis. Dev Cell. 2011; 21:627–41. [PubMed: 21982646]

Finckh U, Xu S, Kumaramanickavel G, Schurmann M, Mukkadan JK, Fernandez ST, John S, Weber JL, Denton MJ, Gal A. Homozygosity mapping of autosomal recessive retinitis pigmentosa locus (RP22) on chromosome 16p12.1-p12.3. Genomics. 1998; 48:341–5. [PubMed: 9545639]

Fortini ME. Notch signaling: the core pathway and its posttranslational regulation. Dev Cell. 2009; 16:633–47. [PubMed: 19460341]

Fromm L, Overbeek PA. Regulation of cyclin and cyclin-dependent kinase gene expression during lens differentiation requires the retinoblastoma protein. Oncogene. 1996; 12:69–75. [PubMed: 8552401]

Hawse JR, DeAmicis-Tress C, Cowell TL, Kantorow M. Identification of global gene expression differences between human lens epithelial and cortical fiber cells reveals specific genes and their associated pathways important for specialized lens cell functions. Mol Vis. 2005; 11:274–83. [PubMed: 15851978]

Inomata H, Haraguchi T, Sasai Y. Robust stability of the embryonic axial pattern requires a secreted scaffold for chordin degradation. Cell. 2008; 134:854–65. [PubMed: 18775317]

Ishibashi M, Ang SL, Shiota K, Nakanishi S, Kageyama R, Guillemot F. Targeted disruption of mammalian hairy and Enhancer of split homolog-1 (HES-1) leads to up-regulation of neural helix-loop-helix factors, premature neurogenesis, and severe neural tube defects. Genes Dev. 1995; 9:3136–48. [PubMed: 8543157]

Jia J, Lin M, Zhang L, York JP, Zhang P. The Notch signaling pathway controls the size of the ocular lens by directly suppressing p57Kip2 expression. Mol Cell Biol. 2007; 27:7236–47. [PubMed: 17709399]

Karsan A. Notch and integrin affinity: a sticky situation. Sci Signal. 2008; 1:pe2. [PubMed: 18270166]

Kok A, Lovicu FJ, Chamberlain CG, McAvoy JW. Influence of platelet-derived growth factor on lens epithelial cell proliferation and differentiation. Growth Factors. 2002; 20:27–34. [PubMed: 11999216]

Kopan R, Ilagan MX. The canonical Notch signaling pathway: unfolding the activation mechanism. Cell. 2009; 137:216–33. [PubMed: 19379690]

Le TT, Conley KW, Brown NL. Jagged 1 is necessary for normal mouse lens formation. Dev Biol. 2009; 328:118–26. [PubMed: 19389370]

Lindsell CE, Boulter J, di Sibio G, Gossler A, Weinmaster G. Expression patterns of Jagged, Delta1, Notch1, Notch2, and Notch3 genes identify ligand-receptor pairs that may function in neural development. Mol Cell Neurosci. 1996; 8:14–27. [PubMed: 8923452]

Lovicu FJ, McAvoy JW. Spatial and temporal expression of p57(KIP2) during murine lens development. Mech Dev. 1999; 86:165–9. [PubMed: 10446277]

Lovicu FJ, McAvoy JW. Growth factor regulation of lens development. Dev Biol. 2005; 280:1–14. [PubMed: 15766743]

Lovicu FJ, McAvoy JW, de Iongh RU. Understanding the role of growth factors in embryonic development: insights from the lens. Philos Trans R Soc Lond B Biol Sci. 2011; 366:1204–18. [PubMed: 21402581]

Mastick GS, Andrews GL. Pax6 regulates the identity of embryonic diencephalic neurons. Mol Cell Neurosci. 2001; 17:190–207. [PubMed: 11161479]

McAvoy JW, Chamberlain CG, de Iongh RU, Hales AM, Lovicu FJ. Lens development. Eye (Lond). 1999; 13(Pt 3b):425–37. [PubMed: 10627820]

McAvoy JW, Chamberlain CG, de Iongh RU, Richardson NA, Lovicu FJ. The role of fibroblast growth factor in eye lens development. Ann N Y Acad Sci. 1991; 638:256–74. [PubMed: 1723855]

McCright B, Lozier J, Gridley T. Generation of new Notch2 mutant alleles. Genesis. 2006; 44:29–33. [PubMed: 16397869]

Medina-Martinez O, Brownell I, Amaya-Manzanares F, Hu Q, Behringer RR, Jamrich M. Severe defects in proliferation and differentiation of lens cells in Foxe3 null mice. Mol Cell Biol. 2005; 25:8854–63. [PubMed: 16199865]

Medina-Martinez O, Jamrich M. Foxe view of lens development and disease. Development. 2007; 134:1455–63. [PubMed: 17344231]

Menko AS, Philip NJ. Beta 1 integrins in epithelial tissues: a unique distribution in the lens. Exp Cell Res. 1995; 218:516–21. [PubMed: 7540985]

Nishimoto S, Kawane K, Watanabe-Fukunaga R, Fukuyama H, Ohsawa Y, Uchiyama Y, Hashida N, Ohguro N, Tano Y, Morimoto T, Fukuda Y, Nagata S. Nuclear cataract caused by a lack of DNA degradation in the mouse eye lens. Nature. 2003; 424:1071–4. [PubMed: 12944971]

Reneker LW, Xie L, Xu L, Govindarajan V, Overbeek PA. Activated Ras induces lens epithelial cell hyperplasia but not premature differentiation. Int J Dev Biol. 2004; 48:879–88. [PubMed: 15558479]

Rosen B, Beddington RS. Whole-mount in situ hybridization in the mouse embryo: gene expression in three dimensions. Trends Genet. 1993; 9:162–7. [PubMed: 8337752]

Rowan S, Conley KW, Le TT, Donner AL, Maas RL, Brown NL. Notch signaling regulates growth and differentiation in the mammalian lens. Dev Biol. 2008; 321:111–22. [PubMed: 18588871]

Saravanamuthu SS, Gao CY, Zelenka PS. Notch signaling is required for lateral induction of Jagged1 during FGF-induced lens fiber differentiation. Dev Biol. 2009; 332:166–76. [PubMed: 19481073]

Schouwey K, Delmas V, Larue L, Zimber-Strobl U, Strobl LJ, Radtke F, Beermann F. Notch1 and Notch2 receptors influence progressive hair graying in a dose-dependent manner. Dev Dyn. 2007; 236:282–9. [PubMed: 17080428]

Simirskii VN, Wang Y, Duncan MK. Conditional deletion of beta1-integrin from the developing lens leads to loss of the lens epithelial phenotype. Dev Biol. 2007; 306:658–68. [PubMed: 17493607]

Stump RJ, Ang S, Chen Y, von Bahr T, Lovicu FJ, Pinson K, de Iongh RU, Yamaguchi TP, Sassoon DA, McAvoy JW. A role for Wnt/beta-catenin signaling in lens epithelial differentiation. Dev Biol. 2003; 259:48–61. [PubMed: 12812787]

Talos F, Schulz R, Moll UM. p63 and canonical Wnt signaling. Cell Cycle. 2010; 9:648–9. [PubMed: 20190579]

Torriglia A, Chaudun E, Chany-Fournier F, Jeanny JC, Courtois Y, Counis MF. Involvement of DNase II in nuclear degeneration during lens cell differentiation. J Biol Chem. 1995; 270:28579–85. [PubMed: 7499373]

Walker J, Menko AS. Integrins in lens development and disease. Exp Eye Res. 2009; 88:216–25. [PubMed: 18671967]

Weinmaster G, Roberts VJ, Lemke G. A homolog of Drosophila Notch expressed during mammalian development. Development. 1991; 113:199–205. [PubMed: 1764995]

Wigle JT, Chowdhury K, Gruss P, Oliver G. Prox1 function is crucial for mouse lens-fibre elongation. Nat Genet. 1999; 21:318–22. [PubMed: 10080188]

Xiong Y, Hannon GJ, Zhang H, Casso D, Kobayashi R, Beach D. p21 is a universal inhibitor of cyclin kinases. Nature. 1993; 366:701–4. [PubMed: 8259214]

Xu L, Overbeek PA, Reneker LW. Systematic analysis of E-, N- and P-cadherin expression in mouse eye development. Exp Eye Res. 2002; 74:753–60. [PubMed: 12126948]

Yoshimoto A, Saigou Y, Higashi Y, Kondoh H. Regulation of ocular lens development by Smad-interacting protein 1 involving Foxe3 activation. Development. 2005; 132:4437–48. [PubMed: 16162653]

Zhang P, Wong C, DePinho RA, Harper JW, Elledge SJ. Cooperation between the Cdk inhibitors p27(KIP1) and p57(KIP2) in the control of tissue growth and development. Genes Dev. 1998; 12:3162–7. [PubMed: 9784491]

Zhu Q, Anderson GW, Mucha GT, Parks EJ, Metkowski JK, Mariash CN. The Spot 14 protein is required for de novo lipid synthesis in the lactating mammary gland. Endocrinology. 2005; 146:3343–50. [PubMed: 15890771]

Zhu Q, Mariash A, Margosian MR, Gopinath S, Fareed MT, Anderson GW, Mariash CN. Spot 14 gene deletion increases hepatic de novo lipogenesis. Endocrinology. 2001; 142:4363–70. [PubMed: 11564699]

Highlights

- Canonical Notch signaling regulates vertebrate lens cell growth and differentiation
- Jagged1 and Rbpj mediate a Notch signal in the lens, but no receptor has been implicated
- Conditional deletion of Notch2 results in excess fiber cell differentiation, but not a loss of proliferation
- Notch2 mutants have increased progenitor cell apoptosis and defective cell cycle withdrawal
- Notch2 is genetically required to maintain Cdh1 and suppress Cdkn1a expression

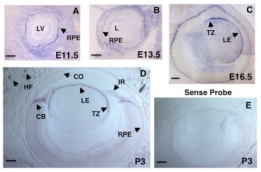

Figure 1. Expression of *Notch2* during eye development

In situ hybridization was used to detect *Notch2* mRNA at embryonic days **A)** 11.5 (E11.5), **B)** 13.5 (E13.5), **C)** 16.5 (E16.5) and **D)** Postnatal day 3 (P3). *Notch2* is expressed consistently in the anterior of the lens vesicle throughout the development. Expression domains become clearly limited to the AEL and transition zone between E16.5 and P3. At P3, ciliary body and hair follicles of the overlying ectoderm show high expression of *Notch2*. **E)** Sense strand hybridization control of P3 section shows absence of hybridization signal in the AEL and transition zone indicating the specificity of the probe used. Scale bars = 100 μM. LV – Lens Vesicle, RPE – Retinal Pigmented Epithelium, LE- Lens Epithelium, TZ – Transition zone, HF- Hair follicle, IR-Iris, CB – Ciliary Body, CO-Cornea.

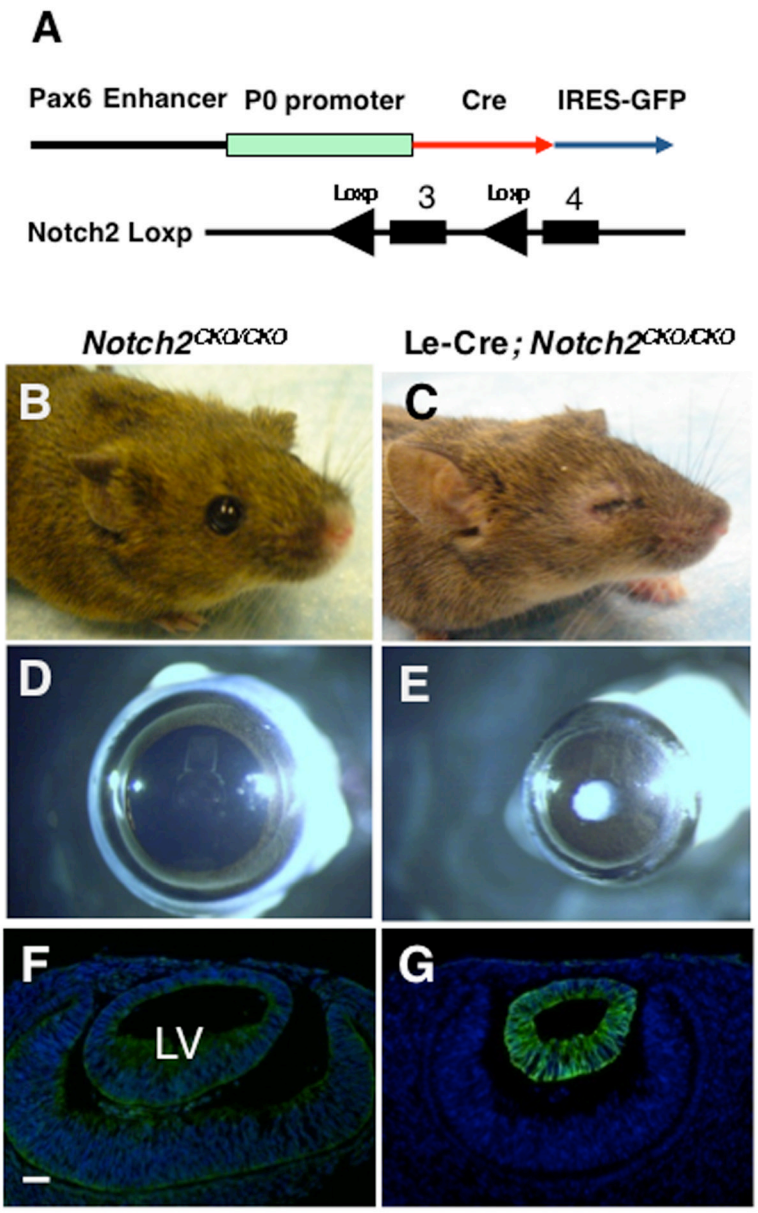

Figure 2. Gross phenotypes of adult Le-Cre; *Notch2*$^{CKO/CKO}$ mice

A) Schematic of the *Cre* driver driven by lens specific Pax6 enhancer and the location of *loxP* sites flanking the exon3 of *Notch2* gene. **B–C)** Gross phenotype of the eye in a 10 week old Le-Cre; *Notch2*$^{CKO/CKO}$ and *Notch2*$^{CKO/CKO}$ control reveals microphthalmia and reduced opening of the eye lids. **D–E)** Le-Cre; *Notch2*$^{CKO/CKO}$ eyeballs have reduced pupillary opening. Cataracts are of frequent occurrence in the Le-Cre; *Notch2*$^{CKO/CKO}$. **F,G)** Anti-GFP/DAPI immunofluorescence staining of E11.5 cryosections of *Notch2*$^{CKO/CKO}$ and Le-Cre; *Notch2*$^{CKO/CKO}$ lenses showing IRES-GFP expression (green) specifically in the lens vesicle (LV) in panel G. Scale bar F,G = 100uM; n = 3 per age and genotype.

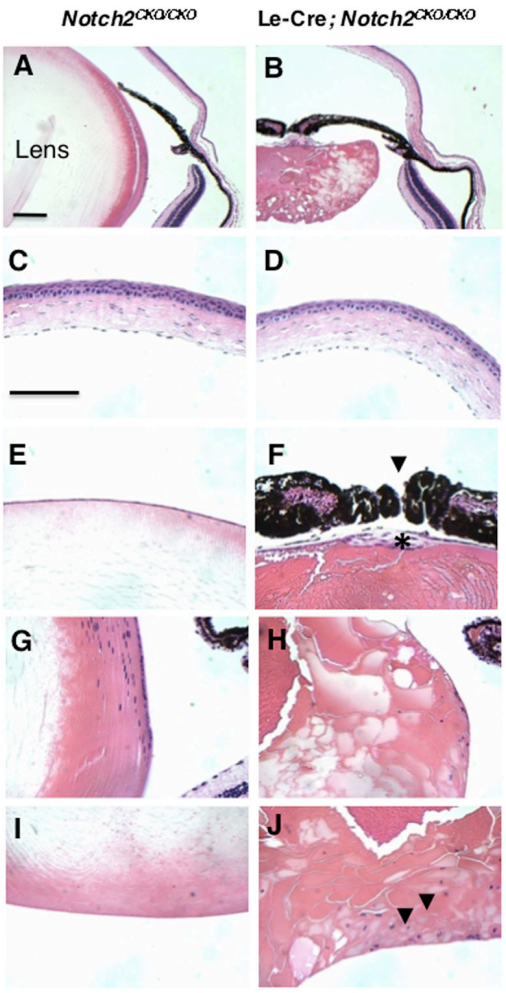

Figure 3. Histological sections through different anterior regions of adult eyes

A–B) Hematoxylin & Eosin (H&E) staining of histological sections of adult eyes (10 weeks old) reveals severe lens defects in the absence of *Notch2*, including disorganized fiber cells and vacuoles. **C–D)** The cornea appears normal in Le-Cre; *Notch2*$^{CKO/CKO}$ and *Notch2*$^{CKO/CKO}$ eyes. **E,F)** Anterior region of the Le-Cre; *Notch2*$^{CKO/CKO}$ lens shows defects in pupillary opening (arrowheads) and denuded Anterior Epithelial Layer (AEL) (asterisk). **G–H)** Bow region of the lens shows disorganized fiber mass in the Le-Cre; *Notch2*$^{CKO/CKO}$. **I–J)** Le-Cre; *Notch2*$^{CKO/CKO}$ posterior lenses reveal abnormal nucleated globular fibers (arrowheads). Scale bar A,B = 20 μM, C–J = 100 μM.

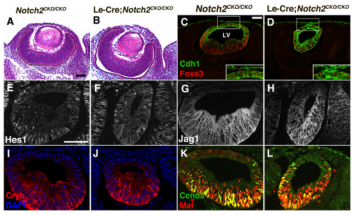

Figure 4. Persistent lens stalks in embryonic Le-Cre; *Notch2*$^{CKO/CKO}$ lenses

A–B) E12.5 histologic sections show relatively normal lens development in *Notch2* mutants, except for a slight reduction in size. **C,D)** Cdh1 (green) and Foxe3 (red) double labeling highlight persistent lens stalks that arise at E11.5. Insets provide a magnified view of the boxed areas. **E–H)** Hes1 expression is reduced in E11.5 *Notch2* conditional mutant lenses, while Jag1 expression seems unaffected. **I,J)** Cryb (red) and DAPI (blue) colabeling indicate fiber cell differentiation initiates on schedule. **K,L)** Ccnd2 (green) and cMaf (red) colabeling further highlight appropriate onset of primary fibergenesis. LV = lens vesicle; scale bar in A,B = 50 μM, C,D = 20 μM and E–L = 20 μM; n = 3 per age and genotype.

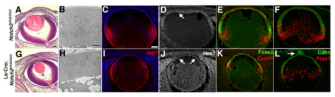

Figure 5. Midgestational phenotypes of Le-Cre; *Notch2*$^{CKO/CKO}$ lenses

A,G) Hematoxylin & Eosin staining of histological sections of E14.5 eyes **B,H)** Electron microscopy images of Le-Cre;*Notch2*$^{CKO/CKO}$ lenses reveals a thinner AEL. **C,I)** Jag1(red) expression marks within the forming transition zone appears to be unaffected in E14.5 *Notch2* lens mutants. **D,J)** Hes1 expression in the AEL (arrows point to Hes1+ nuclei) is essentially abolished by E14.5 in the absence of *Notch2* **E–L)** Foxe3 (green) and Ccnd2 (red) coexpression, as well as Cdh1(green) and Prox1 (red) coexpression demonstrate thinner AEL, anterior shift of transition zone (K) in some mutants, along with inappropriate lens stalks (arrow in L). L = Lens; scale bar in A,G = 100 μM in B,H = 2 μM and C,L = 50 μM; n = 3 per age and genotype.

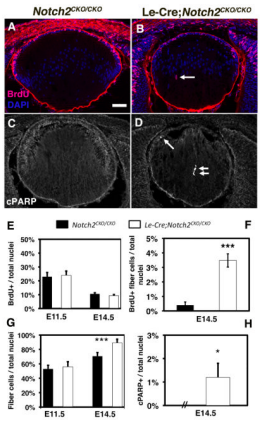

Figure 6. Aberrant proliferation and apoptosis of fiber cells in Le-Cre; *Notch2*$^{CKO/CKO}$ mutant lenses

A,B) E14.5 BrdU pulse-labeled lens cryosections stained with anti-BrdU (red) and DAPI (blue). Arrow in B points to mitotic nucleus in the posterior fiber compartment of a *Notch2* mutant lens. **C,D)** Anti-cPARP labeling of E14.5 lens section highlights excess apoptosis in *Notch2* conditional mutants. **E)** The percentage of pulse-labeled BrdU+ nuclei per total nuclei at E11.5 and E14.5. No significant change was found at either age. **F)** Significantly higher ratio of E14.5 BrdU+/DAPI+ fiber cell nuclei, specifically in the posterior compartment of Le-Cre; *Notch2*$^{CKO/CKO}$ mutant lenses. **G)** The percentage of *Foxe3*-negative cells was determined as a proxy for fiber cells. *Notch2* mutant lenses have more fiber cell nuclei than control lenses at E14.5, but not at E11.5. **H)** In the absence of *Notch2*, there is also an increase in the overall percentage of cPARP+ cells at E14.5. n = 3 per age and genotype; * $p < 0.05$; *** $p < 0.001$; scale bar in A = 50 μM.

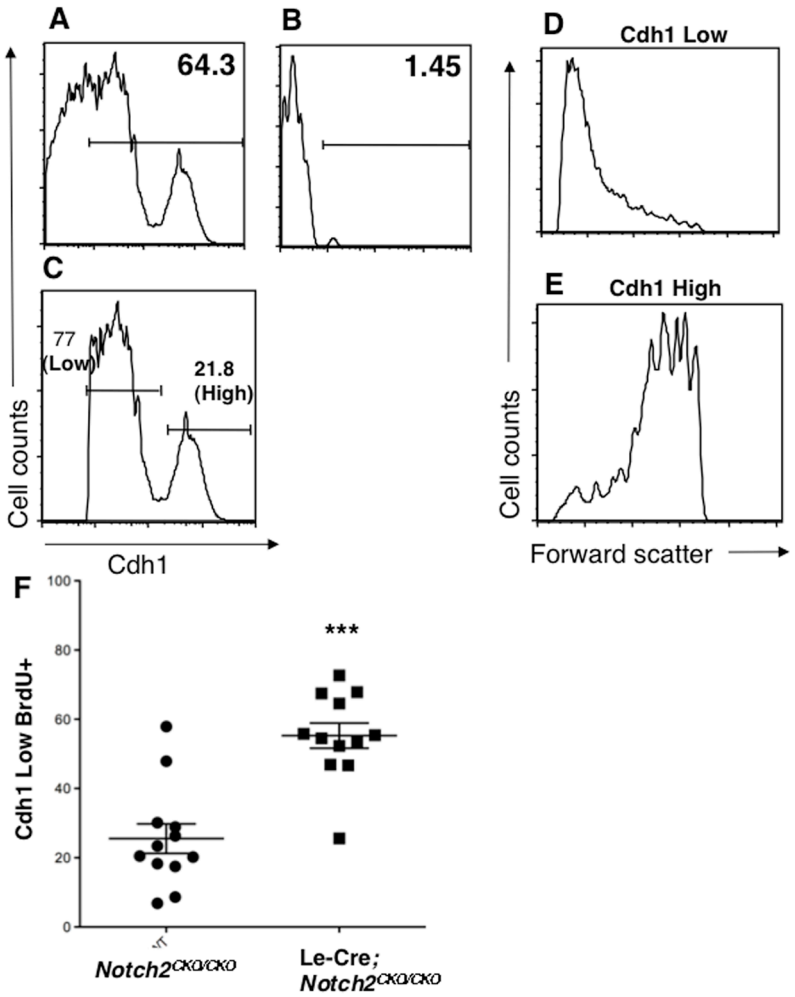

Figure 7. Flow cytometric analysis of E14.5 control and *Notch2* mutant lenses

A,B) Histogram plot of Cdh1+ (E-Cadherin) lens cells, where plot in B is no primary antibody control. **C)** FACS profile of two normal sub-populations of high and low Cdh1-expressing lens cells. Numbers in the plot represent the individual percentages of cells that correspond to the high and low Cdh1+ populations. **D,E)** Peak profiles of forward scatter of low-level Cdh1+ (D) and high level Cdh1+ (E) populations. **F)** Within the low-level Cdh1+ subpopulation, there were significantly more BrdU+ colabeled cells within Le-Cre; *Notch2*$^{CKO/CKO}$ lenses (squares) than for *Notch2*$^{CKO/CKO}$ controls (circles), p = 0.0005 as determined by Mann Whitney test.

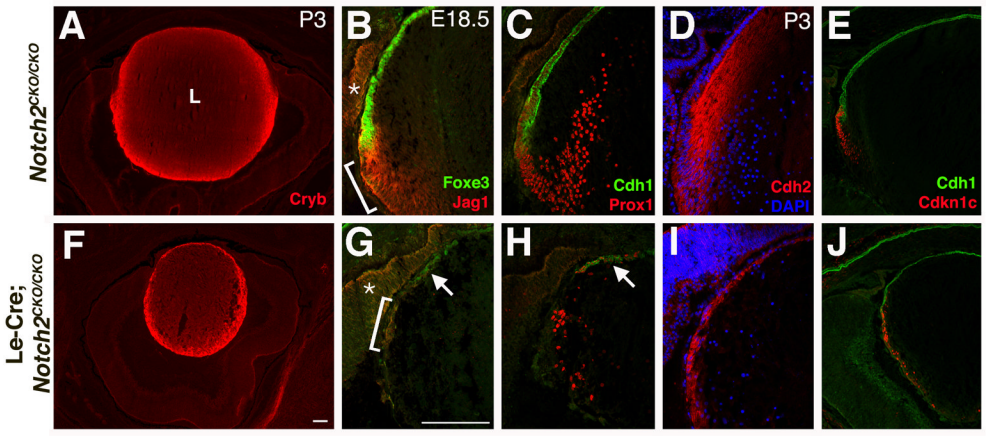

Figure 8. Reduced lens size in Le-Cre; *Notch2*$^{CKO/CKO}$ mutants

A,F) Cryb (β-Crystallin) (red) illustrates a normal pattern of expression but defective fiber cell morphology in P3 *Notch2* mutants. **B,G)** At E18.5 the *Jag1* (red) expression domain within the transition zone (bracketed area) has been dramatically reduced, without *Notch2*. Colabeling with Foxe3 (green) indicates simultaneous loss of AEL cells (arrow in G). Asterisk in both panels marks the ciliary body. **C,H)** Prox1 (red) and Cdh1(green) colabeling at E18.5 reinforces the diminished AEL (arrow points to Cdh1+ cells) and defective transition zone (Prox1+) peripheral cells in *Notch2* mutant lenses. **D,I)** Cdh2 (N-Cadherin) (red) DAPI colabel highlights defective fiber morphology at P3 in the absence of *Notch2*. **E,J)** P3 colabeling of Cdh1+ AEL cells (green) and p57Kip2 (red) differentiating cells further highlight defective AEL and transition zone compartments in Notch2 conditional mutants. L = lens; scale bar in A,F= 50μm, and B–E,G–J =50μm; n =3 per age and genotype.

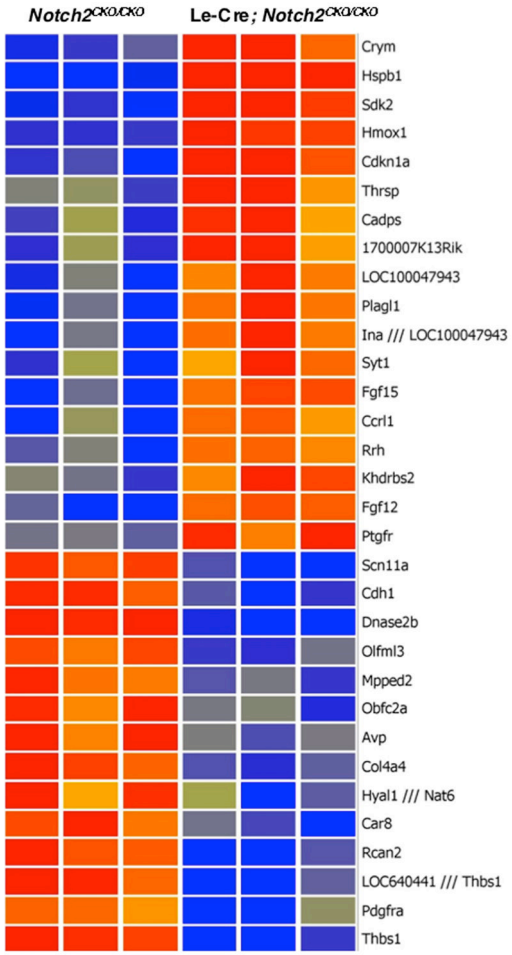

Figure 9. DNA microarray analysis of Control versus Le-Cre*; Notch2*$^{CKO/CKO}$ lenses

Heat map showing fold change patterns of the top differentially expressed genes for E19.5 Le-Cre*; Notch2*$^{CKO/CKO}$ (mutant) and *Notch2*$^{CKO/CKO}$ (control) lenses (fold change ≥ 3 and $p < 0.01$). Three biological replicates per genotype were analyzed using GeneSpring v11.0.2 software. Red represents genes upregulated in the Le-Cre*; Notch2*$^{CKO/CKO}$ lenses, Blue shading represents genes downregulated in the Le-Cre*; Notch2*$^{CKO/CKO}$ lenses. (GEO Accession Number GSE31643).

Table 1

Real Time qPCR analysis of selected genes between control and *Notch2* conditionally mutant lens RNA

Selected genes from the Notch pathway, Wnt pathway and mitotic cell cycle machinery that were differentially expressed between genotypes, and show ≥1.5 fold regulation ($p<0.05$). The minus symbol preceding each fold regulation value represents down regulation within Le-Cre*; Notch2*$^{CKO/CKO}$ lenses.

	Unigene ID	Gene Svmbol	Description	Fold regulation	p value
1	Mm.20894	Trp63	Transformation related protein 63	68.26	0.0302
2	Mm.195663	Cdkn1a	Cyclin-dependent kinase inhibitor 1A (P21)	7.61	0.007
3	Mm.88365	Wnt8b	Wingless related MMTV integration site 8b	7.16	0.0059
4	Mm.4733	Cdkn2a	Cyclin-dependent kinase inhibitor 2A	4.95	0.029
5	Mm.44482	Sfn	Stratifin	2.98	0.0361
6	Mm.10222	Wisp1	WNT1 inducible signaling pathway protein 1	2.34	0.0246
7	Mm.3020	Pparg	Peroxisome proliferator activated receptor gamma	2.33	0.0044
8	Mm.137403	Wnt16	Wingless-related MMTV integration site 16	2.26	0.0008
9	Mm.23608	Sesn2	Sestrin 2	2.24	0.0067
10	Mm.214717	Dkk1	Dickkopf homolog 1 (Xenopus laevis)	2.23	0.0228
11	Mm.38608	Tle2	Transducin-like enhancer of split 2, homolog of Drosophila E(spl)	2.05	0.0095
12	Mm.42095	Sfrp4	Secreted frizzled-related protein 4	2.01	0.0237
13	Mm.31630	Tcf7	Transcription factor 7, T-cell specific	1.9	0.0323
14	Mm.333406	Ccnd2	Cyclin D2	1.76	0.0038
15	Mm.168789	cdkn1c	Cyclin-dependent kinase inhibitor 1c (P57)	1.7	0.0059
16	Mm.184289	Fzd8	Frizzled homolog 8 (Drosophila)	1.68	0.024
17	Mm.278444	Tle1	Transducin-like enhancer of split 1, homolog of Drosophila E(spl)	1.62	0.0038
18	Mm.2444	Myc	Myelocytomatosis oncogene	1.61	0.0447
19	Mm.82598	Dixdc1	DIX domain containing 1	−1.58	0.0199
20	Mm.306946	Wnt7b	Wingless-related MMTV integration site 7B	−1.64	0.0033
21	Mm.281691	Sfrp1	Secreted frizzled-related protein 1	−1.71	0.0336
22	Mm.35605	Cdh1	E-cadherin	−3.07	0.0055
23	Mm.20355	Wnt4	Wingless-related MMTV integration site 4	−4.37	0.0028